TÜBİTAK

Turkish Journal of Earth Sciences

http://journals.tubitak.gov.tr/earth/

Research Article

Turkish J Earth Sci
(2021) 30: 551-560

doi:10.3906/yer-2007-19

Classification of plutonic rock types using thin section images with deep transfer learning

Özlem POLAT[1,*], Ali POLAT[2], Taner EKİCİ[3]

[1]Department of Mechatronic Engineering, Faculty of Technology, Sivas Cumhuriyet University, Sivas, Turkey
[2]Sivas Provincial Disaster and Emergency Directorate, Sivas, Turkey
[3]Department of Geological Engineering, Faculty of Engineering, Sivas Cumhuriyet University, Sivas, Turkey

Received:21.07.2020 • **Accepted/Published Online:** 22.02.2021 • **Final Version:** 16.07.2021

Abstract: Classification of rocks is one of the basic parts of geological research and is a difficult task due to the heterogeneous properties of rocks. This process is time consuming and requires sufficiently knowledgeable and experienced specialists in the field of petrography. This paper has a novelty in classifying plutonic rock types for the first time using thin section images; and proposes an approach that uses the deep learning method for automatic classification of 12 types of plutonic rocks. Convolutional neural network based DenseNet121, which is one of the deep learning architectures, is used to extract the features from thin section images of rocks; and the classification process is carried out with a single layer fully connected neural network. The deep learning model is trained and tested on 2400 images. AUC, accuracy, precision, recall and f1-score are used as performance measure. The proposed approach classifies plutonic rock images on the test set with an average accuracy of 97.52% and a maximum of 98.19%. Thus, the applied deep transfer learning is promising in geosciences and can be used to identify rock types quickly and accurately.

Key words: Rock classification, plutonic rocks, deep transfer learning, DenseNet121, convolutional neural networks

1. Introduction

Rocks in nature are divided into three main classes: sedimentary, metamorphic and igneous. Sedimentary rocks are those that are deposited and lithified at the Earth's surface, with the assistance of running water, wind, ice or living organisms. Most are deposited from the land surface to the bottoms of lakes, rivers, and oceans. Sedimentary rocks are generally stratified. Layers may be distinguished by differences in colour, particle size, type of cement, or internal arrangement. Particularly in clastic sedimentary rocks, the grains are connected to each other by cement material and their grains are composed of quartz, crystal, crystal fragments and rock fragments. Metamorphic rocks are those formed by changes in preexisting rocks under the influence of high temperature, pressure and chemically active solutions. Metamorphic rocks are often formed by processes deep within the Earth that produce new minerals, textures, and crystal structures. The recrystallization that takes place does so essentially in the solid state, rather than by complete remelting, and can be aided by ductile deformation and the presence of interstitial fluids such as water. Metamorphism often produces apparent layering, or banding, because of the segregation of minerals into separate bands. Igneous rocks are those that solidify from magma, a molten mixture of rock-forming minerals and usually volatiles such as gases and steam. Since their constituent minerals are crystallized from molten material, igneous rocks are formed at high temperatures. They originate from processes deep within the Earth typically at depths of about 50 to 200 km in the mid- to lower crust or in the upper mantle. Igneous rocks are subdivided into two categories: plutonic rocks and volcanic rocks in which case the cooling molten material is called lava. Plutonic rocks have formed at considerable depth and have a relatively coarse-grained texture in which the individual crystals can be easily be seen with the naked eye. At the same time, plutonic rocks provide the formation of important mineral deposits. Therefore, they are found together with mineralization zones. Volcanic rocks have been associated with volcanism and have relatively fine grained texture in which most of the individual crystals cannot be seen with the naked eye.

Sedimentary, metamorphic and igneous rocks are grouped into subclasses according to the various characters they have. Identification or classification of the rock types is an important part of geological research. This study focuses on the classification of plutonic rocks.

Rock types can be determined by petrologist with several different methods such as naked eye viewing, microscope examination or chemical analysis. These

* Correspondence: ozlem.polat@cumhuriyet.edu.tr

processes are time consuming and require an experienced human expert who knows the petrographic classification criteria. Identification and classification of rocks can be done effectively and automatically using computer technologies.

In recent years, many researchers have done studies on the classification of rock types, textural identification of rocks, mineral identification in rocks etc. in geoscience using machine learning methods. Marschallinger (1997) studied on mineral classification in macroscopic scale. They applied supervised maximum likelihood classification algorithm; and obtained approximately 90% classification performance. Lepistö et al. (2005) classified the rocks into four groups using k-nearest neighbour (KNN) method as classifier. An image processing and artificial neural network based method proposed by Marmo et al. (2005) for textural identification of carbonate rocks. They classified the textures of carbonate rocks with an accuracy of 93.5%. Rock fragmentation was studied Salinas et al. (2005) using image processing techniques. Singh et al. (2010) studied textural identification of basaltic rock mass using image processing and neural network. They reached 92.22% identification accuracy. Baykan and Yılmaz (2010) made a study on identification of minerals, and they achieved an identification performance of between 80% and 90%. Harinie et al. (2012) classified the rock textures into three main categories i.e. igneous, sedimentary and metamorphic with an accuracy of 87%. Młynarczuk et al. (2013) made a study for classifying nine different types of rock. They applied four pattern recognition techniques: the nearest neighbour, KNN, nearest mode and optimal spherical neighbourhood algorithms. Chatterjee (2013) developed a vision-based rock-type classification model using support vector machine (SVM) algorithm. He classified limestones into six subgroups with 96.2% success rate. Patel and Chatterjee (2016) studied a computer-vision based rock-type classification using probabilistic neural networks. They classified only seven limestone rock types using nine colour histogram features. Joseph et al. (2017) made a study classifying two mineral types in igneous rocks. Tian et al. (2019) classified sand rocks into four subgroups, and they obtained 97% classification accuracy. In some studies on rocks, deep learning methods using convolutional neural network (CNN) have also been applied. Cheng and Guo (2017) identified the rock granularity using CNN. They classified rocks with 98.5% accuracy. Ran et al. (2019) proposed a deep CNN model for classifying six common rock types (granite, limestone, conglomerate, sandstone, shale, mylonite) and they achieved 97.96% classification accuracy. Lime et al. (2019) illustrated the successful classification of microfossils, core images, petrographic photomicrographs, and rock and mineral hand sample images using MobileNetV2 and Inception-V3 from transfer learning models. Transfer learning was also applied for microfossil classification, core description, petrographic analysis, and hand specimen identification by Lima et al. (2019), and applied for classification of cored carbonate rock images by Lima et al. (2019). Another study was conducted by Zhang et al. (2019) using transfer learning. They extracted features from four mineral images (K-feldspar, perthite, plagioclase and quartz) with Inception-V3 architecture, and used machine learning algorithms to identify mineral images. Duarte-Coronado et al. (2019) proposed an innovative technique to estimate porosity in thin section images from the Mississippian strata in the Anadarko basin, Oklahoma (USA). Liu et al. (2019) made a study for recognition of 12 kinds of rock minerals using deep learning. Petrographic analysis based on the microscopic description is a time-consuming and tiring process. To accelerate and automate microfacies classification, Lima et al. (2020) explored the use of deep CNN as a tool. Baraboshkin et al. (2020) used several well-known transfer learning architectures (AlexNet, VGG, GoogleNet, ResNet) for description of rocks. In the study conducted by Koeshidayatullah et al. (2020), the applicability and performance of DCNN-based object detection and image classification approaches were evaluated in terms of carbonate composition analysis. In order to make the precise and intelligent identification of rock types Liu et al. (2020) extracted the features of rock images using simplified VGG16, and classified the rocks using deep CNN with over 80% accuracy rate.

Rock type classification has been handled in all the studies mentioned above; all of them classified different types of rocks from plutonic rocks. To the best of our knowledge, there has been no study systematically classifying plutonic rock types. This paper proposes a new solution for classifying 12 plutonic rock types using thin section images with deep transfer learning. The proposed model achieves high performance in the 12-class rock type classification problem. The main contributions of this paper are as follows: (1) The model proposed in this paper identifies which of the 12 subclasses of plutonic rock types belongs to. Plutonic rocks are classified for the first time. (2) Since a pretrained network is used, classification is performed with less computational load and high performance.

In this study, a deep transfer learning method is used to classify plutonic rock types. 121-layer DenseNet121 architecture as a deep learning model is preferred for solving the 12-class problem. The model, which was created by adding a fully connected layer at the end of DenseNet121 architecture, is applied to a dataset containing 2400 thin section rock images and classification performance of up to 98.19% is achieved.

The remainder of this paper is as follows: Section 2 describes the dataset containing thin section rock images, CNN and DenseNet121 architecture; and performance analyses are also mentioned in this section. In Section 3, the tests and results obtained are given and Section 4 concludes the paper.

2. Materials and methods

2.1. Dataset

Plutonic rocks are formed deep in the ground and over long periods of time, so they show a granular texture consisting of only crystals without any cement or other features. Only clastic sedimentary rocks have crystal fragments, quartz and rock fragments with cement. Mafic mineral content of plutonic rocks is less than 90%. In this study, a total of 2400 images taken from 24 different plutonic rock thin sections were used. Thin sections were obtained from 12 types of plutonic rocks: monzodiorite, granite, quartz syenite, granodiorite, diorite, gabbro, quartz monzonite, monzonite, syenite, alkali-feldspar syenite, alkali-feldspar granite, tonalite (Streckeisen, 1976) (Figure 1).

An example image of each class is shown in Figure 2. Our image data was collected by the Nikon COOLPIX P5100 digital camera system mounted on the top of a Nikon Eclipse 50i POL type binocular research microscope (Nikon Corporation, Tokyo, Japan). In addition, both plane-polarized light and cross-polarized light were used in rock images (100 with plane-polarized light and 100 with cross-polarized light for each rock type class). When obtaining microscope images, the magnification was set to 40× and the illumination setting was never changed. For each of the 12 classes, two thin sections were obtained from two different regions, so 24 thin sections were collected. 100 different images were taken by moving the microscope up and down certain degrees under the same conditions for each 24 rock thin section; totally 2400 images were gathered. Original RGB images were collected at 4000 × 3000 pixels, then resized to 224 × 224 pixels, the size supported by the transfer deep learning network, and used as RGB.

2.2. Convolutional neural networks (CNN)

Deep learning is one of the machine learning methods, and in recent years it has been preferred in various research fields. Deep CNN can automatically extract the features required to classify images, thereby improving classification accuracy and efficiency without further feature selection (Guo et al., 2016).

In recent years, the use of CNNs has increased due to the fact that it can work with huge amounts of data in the fields of research and application; and high accuracy results are obtained. CNN is a robust method used for generally image classification; and the architecture of a

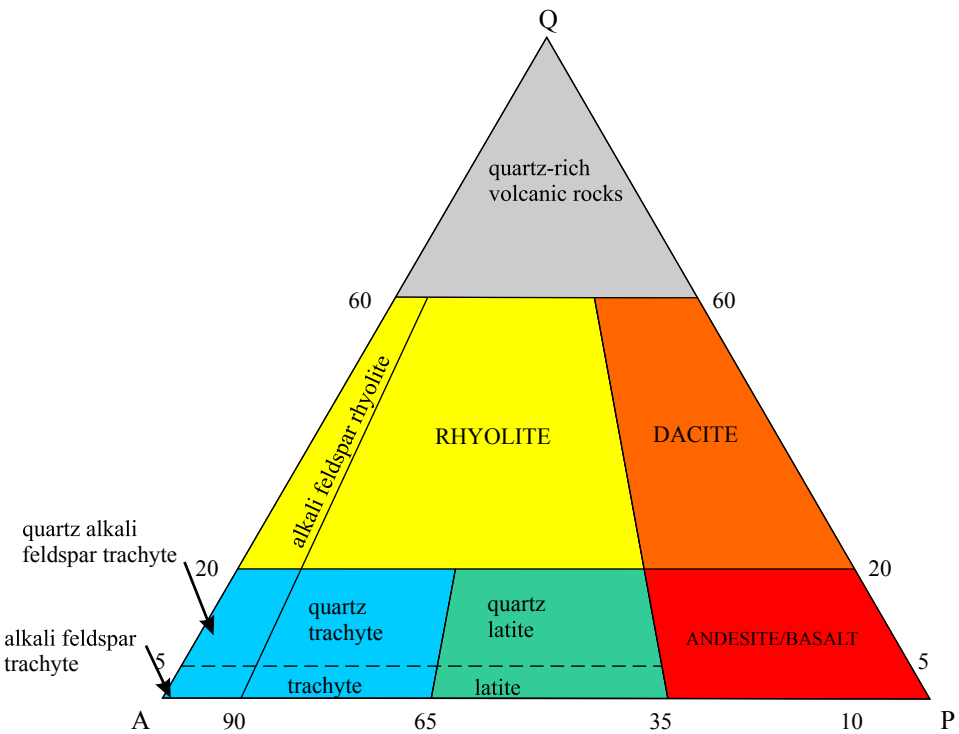

Figure 1. Classification and nomenclature of plutonic rocks according to their modal mineral contents based on (Streckeisen, 1976). (The corners of the triangle are Q = quartz, A = alkali-feldspar, P = plagioclase).

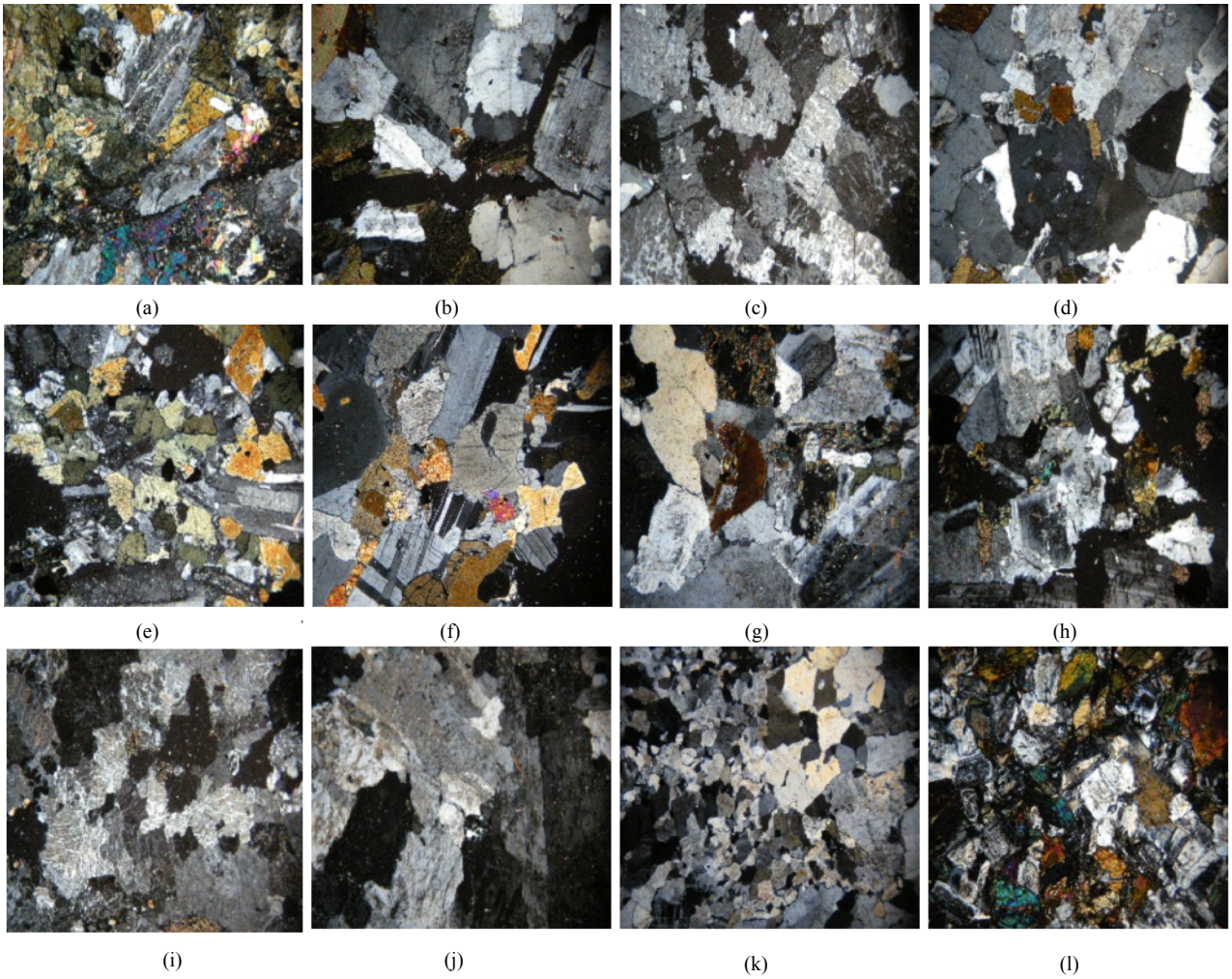

Figure 2. Plutonic rock classes: a) monzodiorite, b)granite, c) quartz syenite, d) granodiorite, e) diorite, f) gabbro, g) quartz monzonite, h) monzonite, i) syenite, j) alkali-feldspar syenite, k)alkali-feldspar granite, l) tonalite.

CNN is similar to the connection model of neurons in the human brain.

Traditional CNN architecture usually includes five main layers: convolution layer, activation layer, pooling layer, flattening layer and fully-connected layer.

The convolution concept was first introduced by LeCun et al. (1989). Convolution is a customized linear process. These networks are simply networks that perform convolution instead of matrix multiplication in at least one layer (Goodfellow et al., 2016). Convolution layer is used to extract features from input images. For this purpose, it is required to slide a filter over the entire image and make some calculations. The filter is a 3-dimensional array like a × b × c and can be of different sizes. Filters create the output data by applying the convolution process to the input images. As a result of this convolution process, an activation map is produced. The structure of the 2D convolution process can be seen in Eq. (1).

$$S(i,j) = (I * K)(i,j) = \sum_{m}\sum_{n} I(i,j)K(i-m, j-n)$$

Given in Eq. (1), I: 2-dimensional image, K: filter matrix shifted on the I image, S: output image, i and j: position of the filter on I during the convolution process, m and n: each position of the filter.

The information from the convolution layer is passed through the activation layer. Activation functions are used as parameters in the activation layer. There are several types of activation functions. The most commonly used of these functions is rectified linear unit (ReLU):

$$R(z) = \max(0, z) \quad (2)$$

$R(z)$ is zero when z is less than zero and $R(z)$ is equal to z when z is above or equal to zero.

The pooling layer is usually used after the activation layer. The primary purpose of using this layer is to reduce the input size (width × height) for the next convolution

layer. The pooling process reveals a value by averaging the values within a specified area, or by calculating the maximum. Various sizes of filters are used in this process.

The penultimate layer is the flattening layer. This layer prepares data for the fully connected layer. Generally, neural networks take input data from a 1-dimensional array. The data in this neural network is the 1-dimensional array of matrices from the convolutional and pooling layer.

The last layer is the fully connected layer in the CNN structure. Fully connected layers are an important component of CNNs, which have proven to be very successful in recognizing and classifying images. The fully connected layer is connected to all neurons in the last convolution layer. This layer helps the network to make final decisions about labelling (classifying) an image.

2.3. DenseNet121 network

Dense Convolutional Network (DenseNet) is one of the pretrained CNN model architectures. Using a pretrained network in classification problems is a very effective approach in the field of deep learning. With the transfer learning, the knowledge extracted from a pretrained model with a lot of data can be used in a new model. There are many advantages of using transfer learning. Its main advantages are that training time is reduced, the accuracy of the neural network is better in most cases, and a lot of data is not required for training. Because the model has already been pretrained, you can build a robust machine learning model with relatively small training data.

DenseNet connects each layer to every other layer in a feed-forward style. While traditional L-layered CNN has L connection, DenseNet has $\frac{L \times (L+1)}{2}$ direct connections. For each layer, feature maps of all previous layers are used as inputs; and each layer's own feature map is also used as input for subsequent layers. DenseNet provides maximum information transfer in the network by directly connecting all layers with each other (Huang et al., 2018).

DenseNet121 consists of four dense blocks. Each dense block contains 6, 12, 24, and 16 convolution blocks; and each convolution block also has two convolution layers, Conv (1 × 1) and Conv (3 × 3), respectively. In addition to these, there are transition blocks between dense blocks. These transition blocks, which are three in total, also have a convolution layer, Conv (1 × 1), and a 2 × 2 average pooling layer. The size of the feature map is changed by downsampling with the pooling layer. Apart from these, there is a convolution layer, Conv (7 × 7), at the input of the network and there is a fully connected convolution layer at the end of the network for classification purpose. Thus, there are 121 convolution layers in the DenseNet network; and therefore it is called as DenseNet121. In DenseNet121 each convolution layer has three consecutive operations: batch normalization (BN), rectified lineer unit (ReLU) and convolution (Conv), respectively (for more information, see Huang et al., 2018). Block diagram related to DenseNet121 can be seen in Figure 3.

2.4. Performance analysis

In this study, features were obtained by DenseNet121 network, and then plutonic rock types were classified by using single layer fully connected neural network. The results obtained from the classification and the actual results determined by the experts were compared in terms of precision (3), recall (4) and f1-score (5).

Consider a classification problem where the results are labeled positive (p) or negative (n); there are four possible outcomes. If the result from an estimate is p and the actual value is p, then this is called true positive (TP); however, if the actual value is n, it is said to be false positive (FP). Conversely, a true negative (TN) occurs when both the predictive result and the actual value were n; and a false negative (FN) occurs when the actual value p is predicted as n.

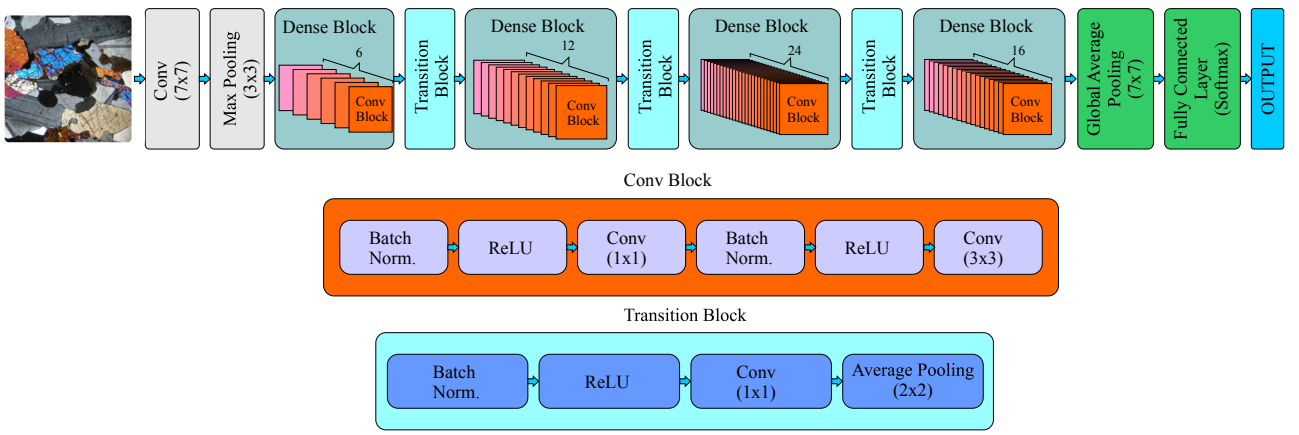

Figure 3. DenseNet121 transfer network. Convolution and transition layer structures.

$$Precision = TP/(TP+FP) \quad (3)$$

$$Recall = TP/(TP+FN) \quad (4)$$

$$F1\text{-}score = 2TP/(2TP+FP+FN) \quad (5)$$

A receiver operating characteristic curve, or ROC curve, is a graphical plot that illustrates classification ability of a classifier as its discrimination threshold is varied. The ROC curve is created by plotting the true positive rate (TPR) against the false positive rate (FPR) at various threshold settings. TPR is the ratio of true positives correctly classified to all positives; and FPR is the ratio of real negatives classified as false positives to all negatives. In this study to evaluate the performance of the classifier the ROC curve for each class is drawn and the AUC value of each class is calculated. AUC is a portion of the area of the unit square, its value will always be between 0 and 1. The closer the value is to 1, the better the classification performance (Fawcett, 2006).

One of the metrics used to measure the performance of the classifier, accuracy is calculated as shown in Eq. (6).

$$Accuracy = \frac{\sum_{i=1}^{12} TP_i}{\sum_{i=1}^{12} TP_i + \sum_{i=1}^{12} FN_i}$$

3. Experimental results and discussion

In the study, Keras[1] and TensorFlow[2] libraries with Python language were used for coding, testing and analysis of the method. DenseNet121, Xception and Inception-V3 architectures were run on the Google Colaboratory (Colab) platform. Colab is a cloud service based on Jupyter Notebooks to apply and popularize machine learning education and research. It provides a fully configured runtime for deep learning and free access to a solid GPU. NVIDIA Tesla T4 GPU with 16GB GDDR GPU memory is used in Colab. The training and test process with the use of the GPU is faster than when using the CPU.

The networks, which were formed to classify plutonic rock types from thin section rock images, were tested on a 12 class dataset consisting of 2400 images. Dataset is randomly divided into training and test sets. 70% of the images were used for training and 30% for test; so 60 images were tested for each rock class. The program guarantees that 70% of each class in the dataset is used in the training set and 30% in the test set. In the fully connected neural network layer, Adadelta (Zeiler, 2012) for DenseNet121, Adam (Kingma and Ba, 2017) for Xception and Inception-V3 are used as optimizer for classification purposes. Transfer learning models were trained five times using training samples with the number of epochs 50 and batch size 16; and then tested with test samples. An epoch elapses an entire training dataset is passed forward and backward through the neural network exactly one time. If the entire training dataset cannot be passed into the algorithm at once, it must be divided into minibatches. Batch size is the total number of training samples present in a single minibatch. In other words, batch size defines number of training samples that going to be propagated through the network. In this study we have 1680 training samples, and batch size is 16, than it will take 105 iterations to complete 1 epoch. The average accuracy and AUC values for DenseNet121, Xception and Inception-V3 were obtained as 97.52%, 90.83%, 85.50% and 0.99, 0.95, 0.92, respectively. Since DenseNet121 gives better results than the other two methods, this study focuses on the DenseNet121 model and its results. So the results related to DenseNet121 obtained from these five experiments are shown in Table 1.

Table 1. Performance of the classifier in terms of AUC and accuracy for each experiment.

Experiment no.	AUC	Accuracy (%)
1	0.99	97.77
2	0.99	97.50
3	0.98	96.94
4	0.99	98.19
5	0.98	97.22
Mean values	0.99	97.52

As seen in Table 1, plutonic rock types are classified with an average of 97.52% and a maximum of 98.19% performance.

Confusion matrix is a frequently used table to describe the performance of a classifier on a test dataset where the true values are known. The confusion matrix for the plutonic rock types classifier having the best classification performance is shown in Table 2. The elements in the diagonal of the confusion matrix show samples that are correctly classified.

In the training of the model with the best classification performance, graphs showing the accuracy and loss of the training according to the number of epoch are shown in Figure 4.

The ROC curve for each rock class of the DenseNet121 architecture with 98.12% classification performance is shown in Figure 5. When the AUC values of the classes are analysed, it is seen that the AUC values of all classes except monzonite are above 0.980. The AUC value of monzonite appears to be 0.957.

[1] Chollet F (2015). Keras [online]. Website https://keras.io [10 May 2021].

[2] Martin A, Agarwal A, Barham P, Brevdo E, Chen Z et al. (2015). TensorFlow: large-scale machine learning on heterogeneous systems [online]. Website tensorflow.org [10 May 2021].

Table 2. Confusion matrix. MD: monzodiorite, Gr: granite, QS: quartz syenite, GD: granodiorite, Di: diorite, Gb: gabbro, QM: quartz monzonite, Mo: monzonite, Sy: syenite, AS: alkali-feldspar syenite, AG: alkali-feldspar granite, Tn: tonalite.

	MD	Gr	QS	GD	Di	Gb	QM	Mo	Sy	AS	AG	Tn
MD	60	0	0	0	0	0	0	0	0	0	0	0
Gr	0	58	0	1	0	0	1	0	0	0	0	0
QS	0	0	59	0	0	0	0	0	0	1	0	0
GD	0	0	0	60	0	0	0	0	0	0	0	0
Di	0	0	0	0	60	0	0	0	0	0	0	0
Gb	0	0	1	0	0	59	0	0	0	0	0	0
QM	0	0	0	1	0	0	58	1	0	0	0	0
Mo	1	1	0	0	0	0	0	55	1	2	0	0
Sy	0	0	0	0	0	0	0	0	60	0	0	0
AS	0	0	1	0	0	0	0	0	0	59	0	0
AG	0	0	0	0	0	0	0	0	0	0	60	0
Tn	0	0	0	0	0	0	0	1	0	0	0	59

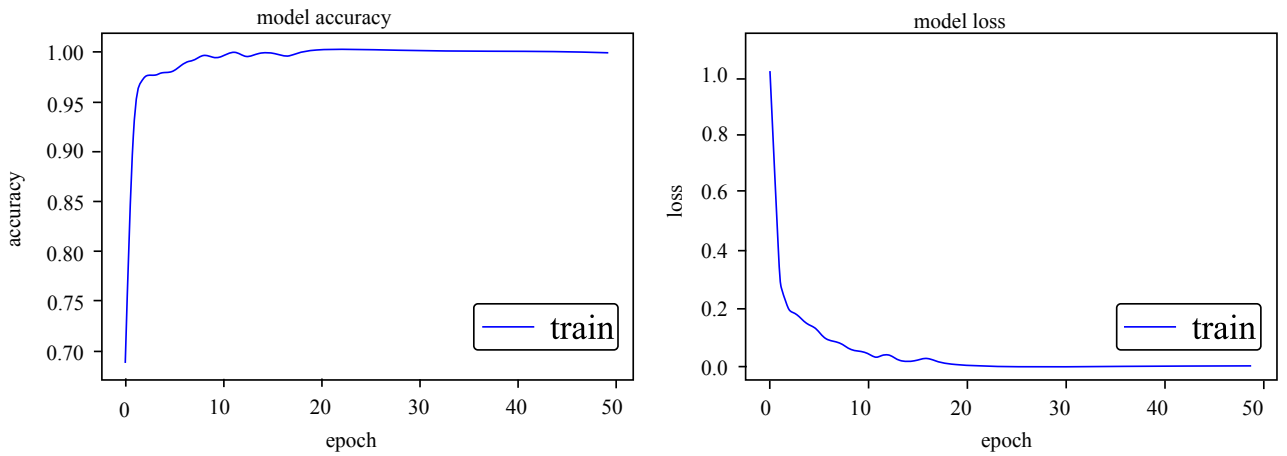

Figure 4. Train accuracy and loss for 50 epochs.

The precision, recall and f1-score values used to evaluate the performance of the classifier are also shown in Table 3 for each rock class. When looking at the recall values, it is seen that five classes (monzodiorite, diorite, granite, syenite, alkali-feldspar granite) are classified with 100% accuracy rate.

The average results of the five experiments conducted in order to better evaluate the performance of the classifier are shown in Table 4. Accordingly, gabbro, alkali-feldspar syenite and alkali-feldspar granite, among the plutonic rock classes, can be classified perfectly. Looking at the other plutonic rock classes, the average performance is at least 95%. These results show how successful transfer learning is also in classifying rocks from thin section images.

There are studies in the literature that classify different rock types with fewer classes, but there is no effective comparison opportunity since there is no study classifying plutonic rock types.

4. Conclusion

In this paper we propose the use of transfer learning for plutonic rock type classification from thin section rock images. Transfer learning uses weights from the network that have been previously trained with millions of data. In this way, it is advantageous to use the transfer learning as it can be used safely with little data and less time spent on training. There are various transfer learning models in the literature. In this study, DenseNet121, Xception and Inception-V3 models were tested. Because it is more successful than other models, DenseNet121 is recommended as a transfer learning method for the classification of plutonic rocks. With the Densenet121

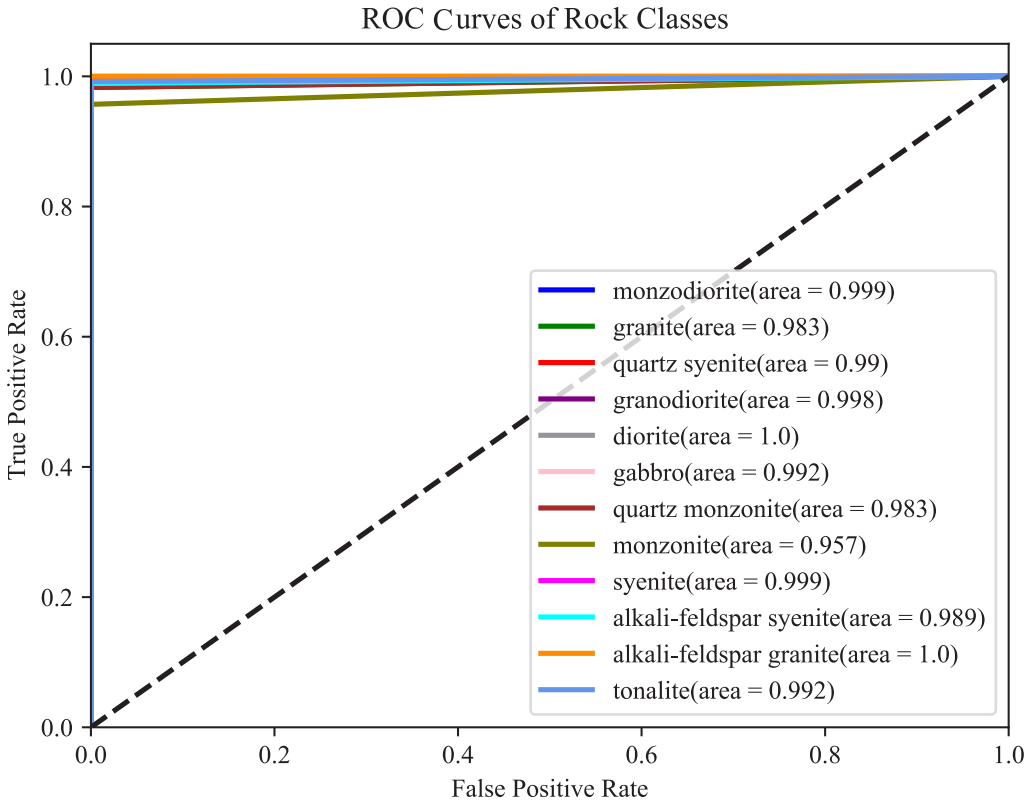

Figure 5. ROC curves and AUC values of each plutonic rock type class for the classifier with 98.19% accuracy rate.

Table 3. Precision, recall and f1-score values of all plutonic rock types for test dataset.

Rock classes	Precision	Recall	F1-score
Monzodiorite	0.98	1.00	0.99
Granite	0.98	0.97	0.97
Quartz syenite	0.97	0.98	0.98
Granodiorite	0.97	1.00	0.98
Diorite	1.00	1.00	1.00
Gabbro	1.00	0.98	0.99
Quartz monzonite	0.98	0.97	0.97
Monzonite	0.96	0.92	0.94
Syenite	0.98	1.00	0.99
Alkali-feldspar syenite	0.95	0.98	0.97
Alkali-feldspar granite	1.00	1.00	1.00
Tonalite	1.00	0.98	0.99

Table 4. Average values of precision, recall, f1-score and AUC related to all plutonic rock types in test dataset.

	Mean			
Rock classes	Precision	Recall	F1-score	AUC
Monzodiorite	0.98	1.00	0.99	0.999
Granite	0.95	0.96	0.96	0.979
Quartz syenite	0.96	0.99	0.98	0.993
Granodiorite	0.96	1.00	0.98	0.996
Diorite	0.99	1.00	1.00	1.000
Gabbro	1.00	0.98	0.99	0.992
Quartz monzonite	0.98	0.90	0.94	0.949
Monzonite	0.95	0.93	0.94	0.965
Syenite	0.98	0.99	0.98	0.995
Alkali-feldspar syenite	0.96	0.96	0.96	0.978
Alkali-feldspar granite	1.00	1.00	1.00	1.000
Tonalite	1.00	0.98	0.99	0.992
Mean values				

network architecture, a maximum of 98.19% and an average of 97.52% performance were achieved in five experiments for the classification of 12 plutonic rock types. Although images with both plane-polarized and cross-polarized light are used together as RGB in the dataset consisting of 2400 images created by us, the classification performance is quite good. When recall averages of 12 plutonic rock types are examined, it is seen that monzodiorite, granodiorite, diorite and alkali-feldspar granite are perfectly classified.

When looking at the literature, no study classifying plutonic type rocks using thin section images has been encountered. Plutonic rock types were classified for the first time with a high performance in this study using thin section images.

In future studies, it is aimed to classify other rock types systematically by using deep learning models.

References

Baraboshkin EE, Ismailova LS, Orlov DM, Zhukovskaya EA, Kalmykov GA et al. (2020).Deep convolutions for in-depth automated rock typing. Computers & Geosciences 135: 104330. doi: 10.1016/j.cageo.2019.104330

Baykan NA, Yılmaz N (2010). Mineral identification using color spaces and artificial neural networks. Computers & Geosciences 36 (1): 91-97. doi: 10.1016/j.cageo.2009.04.009

Chatterjee S (2013).Vision-based rock-type classification of limestone using multi-class support vector machine. Applied Intelligence 39: 14-27. doi: 10.1007/s10489-012-0391-7

Cheng G, Guo W (2017). Rock images classification by using deep convolution neural network. Journal of Physics: Conference Series 887: 1-6.

Duarte-Coronado D, Tellez-Rodriguez J, Lima RPD, Marfurt K, Slatt R (2019). Deep convolutional neural networks as an estimator of porosity in thin-section images for unconventional reservoirs. SEG Technical Program Expanded Abstracts 3181-3184. doi: 10.1190/segam2019-3216898.1

Fawcett T (2006). An introduction to ROC analysis. Pattern Recognition Letters 27 (8): 861-874. doi: 10.1016/j.patrec.2005.10.010

Goodfellow I, Bengio Y, Courville A (2016). Deep Learning. Cambridge, MA, USA: MIT Press.

Guo Y, Liu Y, Oerlemans A, Lao S, Wu S, Lew M (2016). Deep learning for visual understanding: a review. Neurocomputing 187: 27-48. doi: 10.1016/j.neucom.2015.09.116

Harinie T, Janani CI, Sathya BS, Raju S, Abhaikumar V (2012). Classification of rock textures. In: International Conference on Information Systems Design and Intelligent Applications; Visakhapatnam, India. pp. 887-895.

Huang G, Liu Z, Maaten L, Weinberger K (2018). Densely connected convolutional networks. arXiv: 1608.06993v5.

Joseph S, Ujir H, Hipiny I (2017). Unsupervised classification of intrusive igneous rock thin section images using edge detection and colour analysis. In: IEEE International Conference on Signal and Image Processing Applications; Kuching, Malaysia. pp. 530-535. doi: 10.1109/ICSIPA.2017.8120669

Kingma DP, Ba J (2017). Adam: a method for stochastic optimization. arXiv: 1412.6980.

Koeshidayatullah A, Morsilli M, Lehrmann DJ, Al-Ramadan K, Payne JL (2020). Fully automated carbonate petrography using deep convolutional neural networks. Marine and Petroleum Geology 122: 104687. doi: 10.1016/j.marpetgeo.2020.104687

LeCun Y, Boser B, Denker J, Henderson D, Howard R et al. (1989). Backpropagation applied to handwritten zip code recognition. Neural Computation 1 (4): 541-551. doi: 10.1162/neco.1989.1.4.541

Lepistö L, Kunttu I, Visa A (2005). Rock image classification using color features in Gabor space. Journal of Electronic Imaging 14 (4): 1-3. doi: 10.1117/1.2149872

Lima RPD, Bonar A, Coronado DD, Marfurt K, Nicholson C (2019). Deep convolutional neural networks as a geological image classification tool. Sediment Record 17: 4-9. doi: 10.2110/sedred.2019.2.4

Lima RPD, Duarte D, Nicholson C, Slatt R, Marfurt KJ (2020). Petrographic microfacies classification with deep convolutional neural networks. Computers Geosciences 142: 104481. doi: 10.1016/j.cageo.2020.104481

Lima RPD, Marfurt K, Duarte D, Bonar A (2019). Progress and challenges in deep learning analysis of geoscience images. Conference Proceedings, 81st EAGE Conference and Exhibition 2019 (1): 1-5. doi: 10.3997/2214-4609.201901607

Lima RPD, Suriamin F, Marfurt KJ, Pranter MJ (2019).Convolutional neural networks as aid in core lithofacies classification. Interpretation 7 (3): 27-40. doi: 10.1190/INT-2018-0245.1

Liu C, Li M, Zhang Y, Han S, Zhu Y (2019). An enhanced rock mineral recognition method integrating a deep learning model and clustering algorithm. Minerals 9 (9): 516. doi: 10.3390/min9090516

Liu X, Wang H, Jing H, Shao A, Wang L (2020). Research on intelligent identification of rock types based on faster R-CNN method. IEEE Access 8: 21804-21812. doi: 10.1109/access.2020.2968515

Marmo R, Amodio S, Tagliaferri R, Ferreri V, Longo G (2005). Textural identification of carbonate rocks by image processing and neural network: methodology proposal and examples. Computers & Geosciences 31 (5): 649-659. doi: 10.1016/j.cageo.2004.11.016

Marschallinger R (1997). Automatic mineral classification in the macroscopic scale. Computers & Geosciences 23 (1): 119-126. doi: 10.1016/S0098-3004(96)00074-X

Młynarczuk M, G´orszczyk A, ´Slipek B (2013).The application of pattern recognition in the automatic classification of microscopic rock images. Computers & Geosciences 60: 126-133. doi: 10.1016/j.cageo.2013.07.015

Patel A, Chatterjee S (2016). Computer vision-based limestone rock-type classification using probabilistic neural network. Geoscience Frontiers 7 (1): 53-60. doi: 10.1016/j.gsf.2014.10.005

Ran X, Xue L, Zhang Y, Liu Z, Sang X et al. (2019). Rock classification from field image patches analysed using a deep convolutional neural network. Mathematics 7 (8): 755. doi: 10.3390/math7080755

Salinas R, Raff U, Farfan C (2005). Automated estimation of rock fragment distributions using computer vision and its application in mining. IEEE Proceedings - Vision, Image and Signal Processing 152 (1): 1-8. doi: 10.1049/ip-vis:20050810

Singh N, Singh T, Tiwary A, Sarkar K (2010). Textural identification of basaltic rock mass using image processing and neural network. Computational Geosciences 14: 301-310. doi: 10.1007/s10596-009-9154-x

Streckeisen A (1976). To each plutonic rock its proper name. Earth-Science Reviews 12 (1): 1-33. doi: 10.1016/0012-8252(76)90052-0

Tian Y, Guo C, Lv L, Li F, Gao C et al. (2019). Multi-color space rock shin-section image classification with SVM. In: IEEE 8th Joint International Information Technology and Artificial Intelligence Conference; Chongqing, China. pp. 571-574.

Zeiler MD (2012). Adadelta: an adaptive learning rate method. arXiv: 1212.5701. Zhang Y, Li M, Han S, Ren Q, Shi J (2019). Intelligent identification for rock-mineral microscopic images using ensemble machine learning algorithms. Sensors 19 (18): 3914. doi: 10.3390/s19183914